PROCEEDINGS OF SCIENCE

Born–Oppenheimer Effective Theory for multiquark states

Abhishek Mohapatra[a,*]

[a] *Technical University of Munich, TUM School of Natural Sciences, Physics Department, James-Franck-Str. 1, 85748 Garching, Germany.*

E-mail: abhishek.mohapatra@tum.de

The discovery of XYZ exotic states in the hadronic sector, particularly those containing two heavy quarks, remains one of the most intriguing open problems in contemporary particle physics. In this work, we review how the Born–Oppenheimer effective field theory (BOEFT) provides a unified and systematically improvable framework for describing exotic hadrons with atleast two heavy quarks and arbitrary light degrees of freedom such as light quarks or gluons. The BOEFT construction is based on the nonrelativistic QCD expansion and exploits the scale separation and symmetries inherent in systems with two heavy quarks. The framework requires several inputs from lattice QCD. We apply BOEFT to study the spectroscopy of tetraquark and pentaquark candidates such as $\chi_{c1}(3872)$, $T_{cc}(3875)^+$, $P_{cc}(4312)^+$, $P_{cc}(4380)^+$, $P_{cc}(4440)^+$, and $P_{cc}(4457)^+$, as well as their analogues in the bottom sector.

The 42nd International Symposium on Lattice Field Theory (LATTICE2025)
2-8 November 2025
Tata Institute of Fundamental Research, Mumbai, India

*Speaker

PoS(LATTICE2025)064

1. Introduction

The property of color confinement in QCD binds quarks and gluons into color-singlet hadrons and permits a richer spectrum of states beyond conventional hadrons, i.e, mesons and baryons [1, 2]. These include exotic hadrons such as tetraquarks, pentaquarks, hybrids, and glueballs (see Ref. [3] for a review). Over the past two decades, after the discovery of the $\chi_{c1}(3872)$ by the Belle experiment [4], numerous new states located near or above open-flavor thresholds, collectively known as the XYZ exotics have been observed in both the charmonium and bottomonium sectors (see https://qwg.ph.nat.tum.de/exoticshub), whose properties cannot be explained within the conventional quarkonium picture, suggesting more complex multiquark dynamics.

Various phenomenological models such as compact tetraquarks, diquark–antidiquark configurations, hadronic molecules, and hadroquarkonia, have been proposed to interpret XYZ states. However, these approaches rely on ad hoc assumptions and lack a unified connection to QCD, with no single framework describing the full spectrum. In this proceeding, we review the Born–Oppenheimer effective field theory (BOEFT), a QCD-based and systematically improvable framework that describes exotic hadrons without assuming a specific quark configuration. Derived from nonrelativistic QCD, BOEFT leads to coupled-channel Schrödinger equations governing the dynamics. While it requires nonperturbative inputs from lattice QCD such as static potential and generalized Wilson loops, its factorization structure reduces these to a small set of universal, flavor-independent correlators. Through rigorous matching to QCD, BOEFT provides a systematic and model-independent approach to the spectroscopy and production of XYZ states and other multiquark systems.

2. Born-Oppenheimer effective theory

We study hadronic states containing at least two heavy quarks, $Q\bar{Q}$ or QQ, interacting with light degrees of freedom (LDF), namely gluons and light quarks. The relevant energy scales are $m_Q, m_Q v$ ($v \ll 1$), $m_Q v^2$, and $\Lambda_{\rm QCD}$. For nonrelativistic heavy quarks in spatially extended systems such as tetraquarks and pentaquarks, the hierarchy $m_Q \gg m_Q v \sim 1/r \gtrsim \Lambda_{\rm QCD} \gg m_Q v^2$, where r the heavy-quark separation, is parametrically satisfied. This separation of scales suppresses mixing between states split by $O(\Lambda_{\rm QCD})$ and justifies the use of the Born–Oppenheimer (BO) approximation [5], leading to a hierarchy of effective field theories [6]. The resulting low-energy description is the Born–Oppenheimer effective theory (BOEFT) [7–11], which reduces to potential NRQCD for quarkonium [6]. At leading order, BOEFT implements the BO approximation, with heavy quarks moving adiabatically in LDF-induced static potentials depending on their separation $\mathbf{r}$.

At leading order in BOEFT, the dominant contributions arise at $O(1/m_Q)^0$ known as *static approximation*. In this limit, the heavy quarks act as static color sources, while different LDF configurations define different static potentials. The resulting $Q\bar{Q}$ or QQ static potentials are classified according to the representations Λ_η^σ of the cylindrical symmetry group $D_{\infty h}$, which we refer to as the *BO quantum numbers*: $\Lambda \equiv |\lambda| = |\boldsymbol{K}\cdot\hat{\boldsymbol{r}}|$, where $\boldsymbol{K}$ is the total LDF angular momentum. For integer $\Lambda = 0, 1, 2, \ldots \equiv \Sigma, \Pi, \Delta, \ldots$. The index η is the $P\,[C]$ [1] ($g = +1$ and $u = -1$) eigenvalue and $\sigma = \pm 1$ is the reflection eigenvalue, written only for Σ states. The ground state is labeled Λ_η^σ; excited states with the same quantum numbers are labeled as $\Lambda_\eta^{\sigma\prime}, \Lambda_\eta^{\sigma\prime\prime}, \ldots$. In $r \to 0$ limit, the

[1] $P\,[C]$ is defined to be PC for $Q\bar{Q}$ and just P for QQ

PoS(LATTICE2025)064

cylindrical symmetry group is restored to spherical symmetry $O(3)$ $[\times C]$). Consequently, several Λ_η^σ representations become degenerate and reduce to a single $k^{P[C]}$ representation [12]. Assuming that the LDF angular momentum operator $\boldsymbol{K}^2$ has eigenvalues $k(k+1)$, which restricts the projection to $\Lambda \leq k$, we introduce a compact notation for representing LDF states

$$\kappa \equiv \{k^{P[C]}, \text{flavor}\}\,. \tag{1}$$

BOEFT can be derived from NRQCD by integrating out modes of order $m_Q v \gtrsim \Lambda_{\text{QCD}}$ using the nonperturbative quantum matching in [11]. The matching is performed systematically in the in $1/m_Q$ expansion. Retaining at order $1/m_Q$ only the relative kinetic energy, (leading order in v expansion), the BOEFT Lagrangian can be written as

$$L_{\text{BOEFT}} = \int d^3\boldsymbol{R} \int d^3\boldsymbol{r} \sum_{\kappa\lambda\lambda'} \text{Tr}\Bigg\{ \Psi^\dagger_{\kappa\lambda}(\boldsymbol{r},\,\boldsymbol{R},\,t) \Bigg[i\partial_t\,\delta_{\lambda\lambda'} - V_{\kappa,\lambda\lambda'}(r) + \sum_\alpha P^{\alpha\dagger}_{\kappa\lambda}(\theta,\varphi)\,\frac{\boldsymbol{\nabla}^2_r}{m_Q} P^\alpha_{\kappa\lambda'}(\theta,\varphi) \Bigg] \Psi_{\kappa\lambda'}(\boldsymbol{r},\,\boldsymbol{R},\,t) \Bigg\}, \tag{2}$$

where the trace is over color, spin and isospin indices. The fields $\Psi_{\kappa\lambda}$ identify the states while projectors $P^\alpha_{\kappa\lambda}$ projects onto eigenstates of $\mathbf{K}\cdot\hat{\mathbf{r}}$ with eigenvalue λ. Their general expressions in terms of Wigner D-matrices are in [11]. The potentials $V_{\kappa,\lambda\lambda'}(\mathbf{r})$ can be expanded in $1/m_Q$:

$$V_{\kappa\lambda\lambda'}(r) = E^{(0)}_{\kappa,|\lambda|}(r)\delta_{\lambda\lambda'} + \frac{V^{(1)}_{\kappa\lambda\lambda'}(r)}{m_Q} + \ldots\,, \tag{3}$$

where $E^{(0)}_{\kappa,|\lambda|}(r)$ is the static potential (denoted by $E^{(0)}_{\Lambda^\sigma_\eta}(r)$ in the following), and $V^{(1)}_{\kappa\lambda\lambda'}(\mathbf{r})$ includes the leading spin-dependent contributions. The potentials encode the non-perturbative effects from soft degrees of freedom and can be expressed in terms of generalized Wilson loops to be computed on lattice QCD. *In general, potentials carrying the same BO quantum numbers mix* [11, 13].

The equation of motion of the BOEFT Lagrangian in Eq. (2) results in the following radial Schrödinger equation:

$$\sum_\lambda \left[-\frac{1}{m_Q r^2}\partial_r\, r^2 \partial_r + \frac{1}{m_Q r^2}\, M_{\lambda'\lambda} + V_{\kappa\lambda'\lambda} \right] \psi^{(N)}_{\kappa\lambda}(r) = \mathcal{E}_N\, \psi^{(N)}_{\kappa\lambda'}(r)\,, \tag{4}$$

where $\psi^{(N)}_{\kappa\lambda'}(r)$ denotes radial wavefunctions and $N \equiv \{m, j, m_j, l, s\}$ collectively labels the quantum numbers: m is the principal quantum number; $l(l+1)$, $s(s+1)$, and $j(j+1)$ are the eigenvalues of $\boldsymbol{L}^2$, $\boldsymbol{S}^2$, and $\boldsymbol{J}^2$, respectively, with $\boldsymbol{L} = \boldsymbol{L}_Q + \boldsymbol{K}$, $\boldsymbol{S} = \boldsymbol{S}_1 + \boldsymbol{S}_2$, and $\boldsymbol{J} = \boldsymbol{L} + \boldsymbol{S}$; m_j is the eigenvalue of J_3, where $\boldsymbol{L}_Q$ is heavy quark pair orbital angular momentum. In $r \to 0$ limit, static potentials with different $\Lambda = |\lambda|$ but the same κ become degenerate, with splittings arising only at $O\left(r^2\right)$, where $\boldsymbol{K}^2$ symmetry is broken. The mixing matrix $M_{\lambda'\lambda}$ (see Eq. (4.10) of Ref. [11]) has dimension $\min(2k+1,, 2l+1)$ and can be block-diagonalized into sectors of definite parity. Eq (4) thus define the coupled Schrödinger equations for quarkonium, hybrids, doubly heavy baryons, tetraquarks, and pentaquarks, with explicit forms given in Appendix I of Ref. [11]. *Notably, these coupled equations are new for tetraquarks and pentaquarks, while reproducing known results for hybrids and doubly heavy baryons [7, 8, 14].*

3. Born–Oppenheimer Potential: Mixing at short and long distances

Quarkonium and hybrid states contain no light quarks, with gluons as the light degrees of freedom (LDF), whereas tetraquarks and pentaquarks include light quarks and thus carry additional flavor quantum numbers (see Eq. (1)). For $Q\bar{Q}$ tetraquarks and pentaquarks, the $r \to 0$ limit allows both color-singlet and color-octet configurations. In the octet case, the $(Q\bar{Q})_8$ pair combines with LDF in the adjoint representation to form color-singlet hadrons, which we refer to as *adjoint hadrons*. These correspond to tetraquarks $[(Q\bar{Q})_8 + (q\bar{q})_8]$ and pentaquarks $[(Q\bar{Q})_8 + (qqq)_8]$[2].

For doubly heavy tetraquarks $QQ\bar{q}\bar{q}$, the Pauli principle restricts the allowed quantum numbers. In the $r \to 0$ limit, the system forms antitriplet–triplet and sextet–antisextet color configurations. The corresponding LDF states, $(\bar{q}\bar{q})3$ and $(\bar{q}\bar{q})\bar{6}$, combine with $(QQ)_{\bar{3}}$ and $(QQ)_6$, respectively, to produce color-singlet hadrons. However, the $(QQ)_6$ interaction is repulsive at short distances, making such states unlikely to be low-lying [11].

Mixing at short distance: Following Ref. [11], the short-distance behavior of the $\left(Q\bar{Q}\right)_8$ static potential $E^{(0)}_{\Lambda^\sigma_\eta}(r)$ can be written as

$$E_{(\Lambda)_\eta}(r) = V_o(r) + \Lambda_\kappa + O(r^2). \tag{5}$$

where $V_o(r) = \alpha_s/(6r)$ is the color octet potential and Λ_κ is the adjoint hadron mass. Eq. (5) shows that at leading order in the multipole expansion, multiple static potentials with different BO quantum numbers, but with the same κ quantum numbers become degenerate in $r \to 0$ limit and hence mix. Similarly, in the (QQ) case, we get

$$E^{(0)}_{(\Lambda)_\eta}(r) = V_l(r) + \Lambda^l_\kappa + O(r^2), \qquad l = (T, \Sigma) \tag{6}$$

where $V_T(r) = -2\alpha_s/(3r)$ and $V_\Sigma = \alpha_s/(3r)$ is the color triplet and sextet potentials respectively and Λ^l_κ is either triplet or sextet hadron mass. The degeneracy is broken by the $O\left(r^2\right)$ terms [6].

$k^P_{\bar{q}} \otimes k^P_q$	k^{PC}	BO quantum # Λ^σ_η
$(1/2)^- \otimes (1/2)^+$	0^{-+}	Σ^-_u
	1^{--}	Σ^+_g, Π_g

$k^P_{\bar{q}} \otimes k^P_{\bar{q}}$	k^P	BO quantum # Λ^σ_η
$(1/2)^- \otimes (1/2)^-$	0^+	Σ^+_g
	1^+	Σ^-_g, Π_g

Table 1: The $k^{P[C]}$ and corresponding BO Λ^σ_η quantum numbers shown in third column of the light $\bar{q}q$ (left) and $\bar{q}\bar{q}$ (right) pairs for the lowest light quark states contributing to S-wave plus S-wave heavy-light $Q\bar{q} - \bar{Q}q$ and $Q\bar{q} - Q\bar{q}$ thresholds, respectively.

Mixing at long distance: The large-distance behavior of static potentials depends on the LDF. In the quenched approximation, quarkonium ($k^{PC} = 0^{++}$, Σ^+_g) and the lowest hybrid ($k^{PC} = 1^{+-}$, Σ^-_u, Π_u) static potentials rise linearly with r. For tetraquarks and pentaquarks, where LDF include light quarks, one must instead consider open-flavor (heavy–light) thresholds, whose BO quantum numbers Λ^σ_η are listed in Tables 1 and 2. *Conservation of Λ^σ_η implies that BOEFT potentials with adjoint-hadron behavior at short distances (Eq. (5)) asymptotically approach the corresponding heavy–light thresholds—$(Q\bar{q})(\bar{Q}q)$ for tetraquarks and $(Qqq)(\bar{Q}q)$ for pentaquarks [11, 18], with*

[2]Lattice QCD indicates that color-singlet configurations are not sufficiently bound to form multiquark states [15–17].

analogous behavior for $QQ\bar{q}\bar{q}$ systems. Whether bound states form depends on how these potentials approach the thresholds, offering a dynamical explanation for no experimental observation of excited tetraquark or pentaquark multiplets [18]. Additionally, in the unquenched case, the string breaking

$k^P_{qq} \otimes k^P_q$	k^P	BO quantum # $D_{\infty h}$
$0^+ \otimes (1/2)^+$	$(1/2)^+$	$(1/2)_g$
$1^+ \otimes (1/2)^+$	$(1/2)^+$	$(1/2)_g$
	$(3/2)^+$	$\{(1/2)'_g, (3/2)_g\}$

Table 2: The total LDF spin-parity k^P and corresponding BO quantum numbers shown in third column of light $qq \otimes q$ combinations for the lowest light quark states contributing to S-wave plus S-wave heavy-light $Qqq - \bar{Q}q$ thresholds. The first row is for $\Lambda_c \bar{D}$ or $\Lambda_b \bar{B}$ thresholds with isospin $I = 1/2$, while the second and third rows are for the $\Sigma_c \bar{D}$ or $\Sigma_b \bar{B}$ thresholds, and include both isospin $I = 1/2$ and $I = 3/2$.

induces mixing between quarkonium or hybrid static potentials and heavy–light threshold states, governed by the BO quantum numbers Λ^σ_η [11]. In such case, the eigenvalues of the potential matrix are called *adiabatic potentials*. The possible behaviors of the lowest static potentials in the isospin $I = 1$ sector are illustrated in first two skectches of Fig. 1. In particular, depending on the behavior of the Π_g potential at intermediate distances, the potential may or may not support a bound state. The string breaking and behavior of the lowest static potentials in the isospin $I = 1$ sector is shown in bottom sktech of Fig. 1.

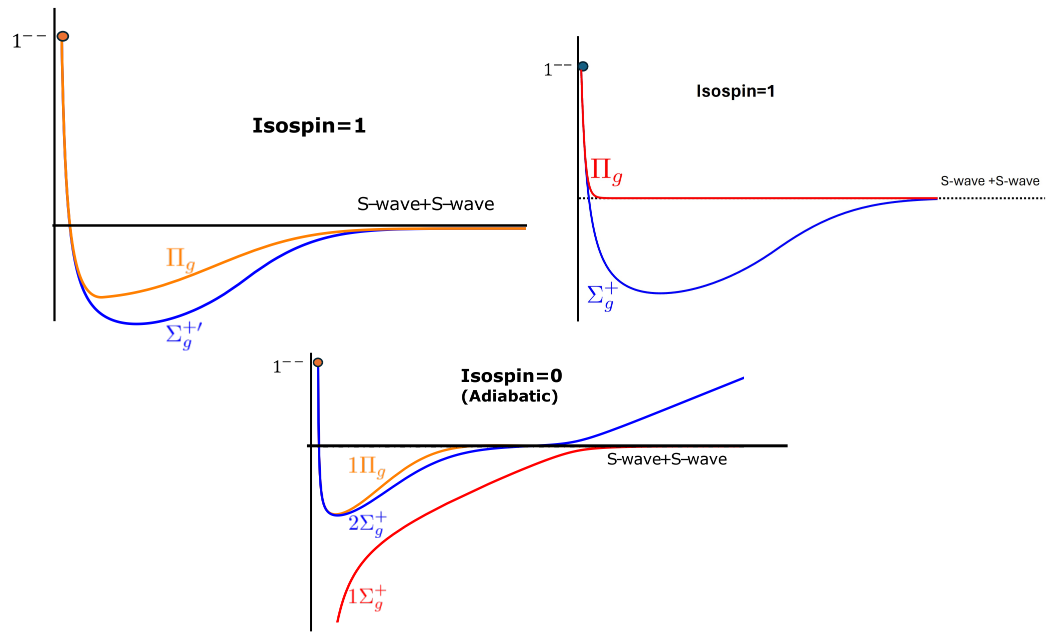

Figure 1: Top: Examples of $I = 1$ tetraquark static potentials approaching S-wave heavy–light thresholds, where the evolution of the Π_g potential determines whether bound states are supported. Bottom: The lowest $I = 0$ $Q\bar{Q}$ adiabatic potentials, showing avoided level crossing between the quarkonium Σ_g^+ and tetraquark $\Sigma_g^{+\prime}$. In the $r \to 0$ limit, the tetraquark potential is repulsive, consistent with adjoint-hadron behavior. The string-breaking radius is $r_c \sim 1.2$ fm, where the avoided crossing occurs [19, 20].

4. Tetraquarks: χ_{c1} (3872) & T_{cc} $(3875)^+$ and Pentaquarks

$Q\bar{Q}$ color state	$q\bar{q}$ spin k^{PC}	BO quantum # Λ_η^σ	l	J^{PC} $\{S=0, S=1\}$	Multiplets
Octet **8**	0^{-+}	Σ_u^-	0	$\{0^{++}, 1^{+-}\}$	T_1^0
			1	$\{1^{--}, (0,1,2)^{-+}\}$	T_2^0
	1^{--}	$\Sigma_g^{+\prime}, \Pi_g$	1	$\{1^{+-}, (0,1,2)^{++}\}$	T_1^1
		$\Sigma_g^{+\prime}$	0	$\{0^{-+}, 1^{--}\}$	T_2^1
		Π_g	1	$\{1^{-+}, (0,1,2)^{--}\}$	T_3^1

Table 3: J^{PC} multiplets for the lowest $Q\bar{Q}q\bar{q}$ [11], with Λ_η^σ listed in the third column. Multiplets are labeled as T_i^k in the last column in increasing energy order.

$\chi_{c1}(3872)$ **and** X_b**:** The first observed XYZ state was the $\chi_{c1}(3872)$, discovered by Belle [4]. It has $J^{PC} = 1^{++}$, isospin $I = 0$, and is likely a $c\bar{c}q\bar{q}$ state ($q = u, d$), with a mass within ~ 100 keV of the $D^{*0}\bar{D}^0$ threshold [21]. We identify it as the 1^{++} ($I = 0$) member of the lowest $k^{PC} = 1^{--}$ multiplet (Table 3). Including short- and long-distance mixing among the tetraquark potentials $\Sigma_g^{+\prime}$, Π_g, and the quarkonium Σ_g^+, the coupled Schrödinger equations are:

$$\left[-\frac{1}{m_Q r^2}\,\partial_r r^2 \partial_r + \frac{1}{m_Q r^2}\begin{pmatrix} l\,(l+1) & 0 & 0 \\ 0 & l(l+1)+2 & -2\sqrt{l(l+1)} \\ 0 & -2\sqrt{l(l+1)} & l(l+1) \end{pmatrix} + \begin{pmatrix} V_{\Sigma_g^+}(r) & V_{\Sigma_g^+-\Sigma_g^{+\prime}}(r) & 0 \\ V_{\Sigma_g^+-\Sigma_g^{+\prime}}(r) & V_{\Sigma_g^{+\prime}}(r) & 0 \\ 0 & 0 & V_{\Pi_g}(r) \end{pmatrix}\right]\begin{pmatrix} \psi^{(N)}_{\Sigma_g} \\ \psi^{(N)}_{\Sigma_g'} \\ \psi^{(N)}_{\Pi_g} \end{pmatrix} = \mathcal{E}_N \begin{pmatrix} \psi^{(N)}_{\Sigma_g} \\ \psi^{(N)}_{\Sigma_g'} \\ \psi^{(N)}_{\Pi_g} \end{pmatrix}, \quad (7)$$

$V_{\Sigma_g^+}(r)$, $V_{\Sigma_g^{+\prime}}(r)$, $V_{\Pi_g}(r)$, and the mixing $V_{\Sigma_g^+-\Sigma_g^{+\prime}}(r)$ are obtained from lattice QCD [19, 20] and constrained by BO symmetry in the $r \to 0$ and $r \to \infty$ limits. The adiabatic potentials (Fig. 1) follow from diagonalizing Eq. (7). Including spin splittings, either from lattice hybrid results or via first-order perturbation theory in the heavy–light threshold splitting, yields a 1^{++} state just below the $D\bar{D}^*$ threshold, which is identified with $\chi_{c1}(3872)$. The remaining multiplet consists of a 1^{+-} state at 3957(11) MeV, a 0^{++} state at 3846(11) MeV, and a 2^{++} state at 4004(14) MeV (Fig. 2), along with a more deeply bound $\chi_{c1}(1P)$ at 3537 MeV. *Notably,* $\chi_{c1}(3872)$ *is distinct from the conventional* $\chi_{c1}(2P)$ *charmonium state despite having the same* $J^{PC} = 1^{++}$.

The $\chi_{c1}(3872)$ has a large scattering length of ~ 15 fm and is predominantly a tetraquark state, with a small quarkonium component around $|\psi_{\Sigma_g^+}|^2 \approx 8\%$, and tetraquark components $|\psi_{\Sigma_g^{+\prime}}|^2 \approx 38\%$ and $|\psi_{\Pi_g}|^2 \approx 54\%$. Although the mixing from the narrow avoided level crossings is small and has limited impact on the spectrum, still it is useful for describing decays to open-flavor threshold states [23–26]. A similar analysis in the bottomonium sector yields results shown in Fig. 2.

The $T_{cc}^+(3875)$ **and** T_{bb} **states.** The doubly charmed tetraquark $T_{cc}^+(3875)$, discovered by LHCb in 2021 [27, 28], has favored quantum numbers $I = 0$ and $J^P = 1^+$ and is consistent with a $cc\bar{u}\bar{d}$ configuration. It is the longest-lived exotic state observed so far, with $\Gamma \approx 50$ keV, and lies about 360 keV below the $D^{*+}D^0$ threshold. We identify it as the 1^+ ($I = 0$) member of the lowest $k^P = 0^+$ ("good diquark") multiplet (Table 4). In BOEFT, $T_{cc}^+(3875)$ is described by a single radial

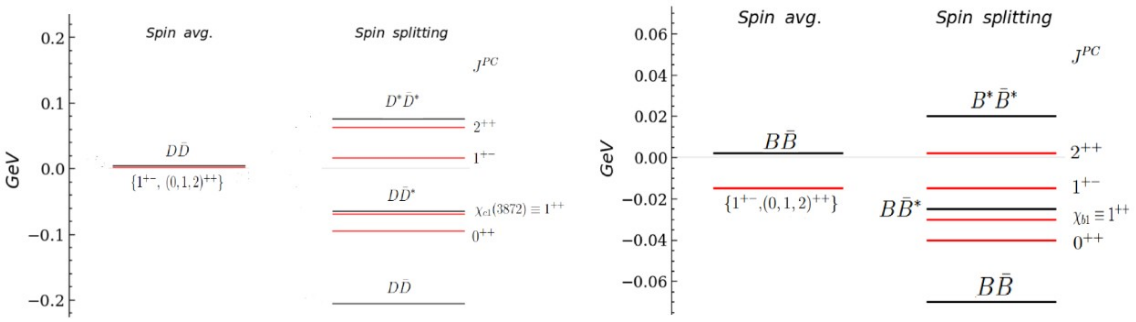

Figure 2: Lowest $Q\bar{Q}q\bar{q}$ spectrum in charm and bottom sectors (red lines) vs thresholds (black lines) [22].

QQ color state	$\bar{q}\bar{q}$ spin k^P	BO quantum # Λ_η^σ	Isospin I	l	J^P $S=0$	J^P $S=1$
Antitriplet $\bar{3}$	0^+	Σ_g^+	0	0	—	1^+
				1	1^-	—
	1^+	Σ_g^-, Π_g	1	0	0^-	—
				1	1^-	$(0,1,2)^+$

Table 4: J^P multiplets for the lowest $QQ\bar{q}\bar{q}$ tetraquarks.

Schrödinger equation with the Σ_g^+ potential, which approaches a 0^+ triplet-meson (good diquark) configuration at $r \to 0$ and a meson–meson threshold at $r \to \infty$ [11]:

$$\left[-\frac{1}{m_Q r^2}\,\partial_r\, r^2\, \partial_r + \frac{l(l+1)}{m_Q r^2} + V_{\Sigma_g^+}(r)\right]\psi_{\Sigma_g^+}^{(N)} = \mathcal{E}_N\, \psi_{\Sigma_g^+}^{(N)}, \tag{8}$$

where $V_{\Sigma_g^+}(r)$ can be extracted from lattice QCD [29, 30]. Tuning the triplet meson 0^+ mass to $\Lambda_{0^+}^t = 664$ MeV and solving Eq. (8), we get a state 323 keV below the DD^* threshold, with scattering length of about 8 fm, that we identify with $T_{cc}^+(3875)$ [22]. Performing a similar analysis in the bb or bc sectors with $\Lambda_{0^+}^t = 664$ MeV, we get a T_{bb} and T_{bc} states around 115 MeV and 25 MeV, respectively below the corresponding thresholds. These results are consistent with different lattice QCD calculations [22].

Pentaquarks: The hidden-charm pentaquark states $P_{c\bar{c}}\,(4312)^+$, $P_{c\bar{c}}\,(4380)^+$, $P_{c\bar{c}}\,(4440)^+$, and $P_{c\bar{c}}\,(4457)^+$ with quark content $c\bar{c}qqq$, where $q = (u,d)$, all with isospin $I = 1/2$ and unknown J^P, were discovered by LHCb [31, 32]. The coupled channel Schroedinger equations are given by Eqs. (3.6) and (3.7) in [26]. There are two adjoint baryons $\Lambda_{(1/2)^+}$ and $\Lambda_{(3/2)^+}$. Their values $\Lambda_{(1/2)^+}^b \approx 1125$ MeV and $\Lambda_{(3/2)^+}^b \approx 1152$ MeV are tuned to reproduce the masses of $P_{c\bar{c}}\,(4312)^+$, and $P_{c\bar{c}}\,(4380)^+$ and also decays to J/ψ. The multiplet is given in Table 5 and the spectrum is shown in Fig. 3.

5. Conclusions

The Born–Oppenheimer EFT (BOEFT) provides a systematic QCD-based framework to describe multiquark hadrons with at least two heavy quarks. Its main limitation lies in the incomplete knowledge of the potentials entering the coupled Schrödinger equations, which must be determined

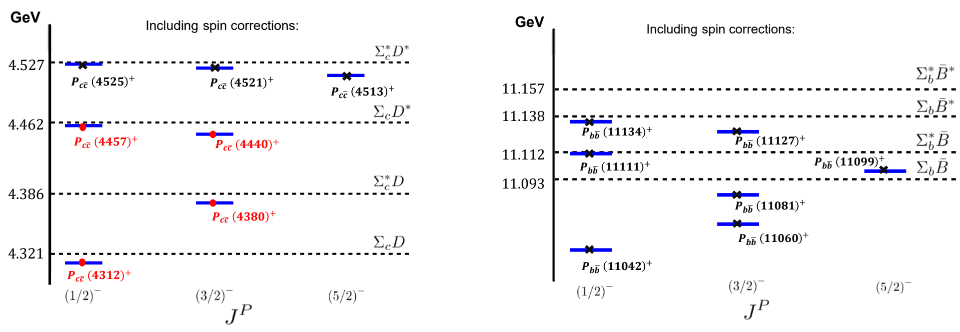

Figure 3: Pentaquark spectrum in charm and bottom sectors [26].

$Q\bar{Q}$ color state	Light spin k^P	BO quantum # $D_{\infty h}$	l	J^P $\{s=0, s=1\}$
Octet	$(1/2)^+$	$(1/2)_g$	1/2	$\{1/2^-, (1/2, 3/2)^-\}$
8	$(3/2)^+$	$\{(1/2)'_g, (3/2)_g\}$	3/2	$\{3/2^-, (1/2, 3/2, 5/2)^-\}$

Table 5: J^P multiplets for the lowest $Q\bar{Q}qqq$ pentaquarks [11].

from lattice QCD. While there are numerous lattice determinations of hybrid static potentials, tetraquark and pentaquark potentials are still under active investigation. Accurate knowledge of these potentials is essential for discriminating among scenarios and for explaining dynamically why some states exist while others do not. We showed applications of BOEFT to the tetraquark and pentauqark spectrum. Applications to tetraquark and pentaquark spectra suggest that only the lowest-lying Born–Oppenheimer potentials may support bound states, potentially explaining the observed scarcity of such states compared to naive expectations of quark combinations. *Notably, the BO framework does not assume a specific internal structure (e.g., compact tetraquark or molecule); instead, the coupled Schrödinger equations determine the composition, binding energies, and spatial structure of the states.*

More recently, BOEFT has been extended to inclusive hadroproduction of $\chi_{c1}(3872)$ and pentaquarks [33], yielding upper bounds on cross sections through factorization of long-distance matrix elements into a universal nonperturbative parameter and the wavefunction at the origin.

Acknowledgments

I thank Matthias Berwein, Nora Brambilla, Antonio Vairo, and Tommaso Scirpa for collaboration on the work presented here.

References

[1] M. Gell-Mann, *A Schematic Model of Baryons and Mesons*, *Phys. Lett.* **8** (1964) 214.

[2] G. Zweig, *Developments in the quark theory of hadrons*, *CERN Report No.8182/TH.401, CERN Report No.8419/TH.412* (1964) .

[3] N. Brambilla, S. Eidelman, C. Hanhart, A. Nefediev, C.-P. Shen, C. E. Thomas et al., *The XYZ states: experimental and theoretical status and perspectives*, *Phys. Rept.* **873** (2020) 1 [1907.07583].

[4] Belle collaboration, *Observation of a narrow charmonium-like state in exclusive $B^{\pm} \to K^{\pm}\pi^{+}\pi^{-}J/\psi$ decays*, *Phys. Rev. Lett.* **91** (2003) 262001 [hep-ex/0309032].

[5] M. Born and R. Oppenheimer, *Zur quantentheorie der molekeln*, *Annalen der Physik* **389** (1927) 457 [https://onlinelibrary.wiley.com/doi/pdf/10.1002/andp.19273892002].

[6] N. Brambilla, A. Pineda, J. Soto and A. Vairo, *Effective Field Theories for Heavy Quarkonium*, *Rev. Mod. Phys.* **77** (2005) 1423 [hep-ph/0410047].

[7] M. Berwein, N. Brambilla, J. Tarrús Castellà and A. Vairo, *Quarkonium Hybrids with Nonrelativistic Effective Field Theories*, *Phys. Rev. D* **92** (2015) 114019 [1510.04299].

[8] R. Oncala and J. Soto, *Heavy Quarkonium Hybrids: Spectrum, Decay and Mixing*, *Phys. Rev. D* **96** (2017) 014004 [1702.03900].

[9] N. Brambilla, G. a. Krein, J. Tarrús Castellà and A. Vairo, *Born-Oppenheimer approximation in an effective field theory language*, *Phys. Rev. D* **97** (2018) 016016 [1707.09647].

[10] J. Soto and J. Tarrús Castellà, *Nonrelativistic effective field theory for heavy exotic hadrons*, *Phys. Rev. D* **102** (2020) 014012 [2005.00552].

[11] M. Berwein, N. Brambilla, A. Mohapatra and A. Vairo, *Hybrids, tetraquarks, pentaquarks, doubly heavy baryons, and quarkonia in Born-Oppenheimer effective theory*, *Phys. Rev. D* **110** (2024) 094040 [2408.04719].

[12] UKQCD collaboration, *Hadrons with a heavy color adjoint particle*, *Phys. Rev. D* **59** (1999) 094509 [hep-lat/9811010].

[13] A. Mohapatra, *One Born Oppenheimer Effective Theory to rule all Exotics*, *PoS* **QCHSC24** (2025) 140 [2503.22847].

[14] J. Soto and J. Tarrús Castellà, *Effective field theory for double heavy baryons at strong coupling*, *Phys. Rev. D* **102** (2020) 014013 [2005.00551].

[15] M. Alberti, G. S. Bali, S. Collins, F. Knechtli, G. Moir and W. Söldner, *Hadroquarkonium from lattice QCD*, *Phys. Rev. D* **95** (2017) 074501 [1608.06537].

[16] S. Prelovsek, H. Bahtiyar and J. Petkovic, *Zb tetraquark channel from lattice QCD and Born-Oppenheimer approximation*, *Phys. Lett. B* **805** (2020) 135467 [1912.02656].

[17] Y. Lyu, T. Doi, T. Hatsuda and T. Sugiura, *NJ/ψ and $N\eta_c$ interactions from lattice QCD*, *PoS* **LATTICE2024** (2025) 103 [2502.00054].

PoS(LATTICE2025)064

[18] E. Braaten and R. Bruschini, *Exotic hidden-heavy hadrons and where to find them*, *Phys. Lett. B* **863** (2025) 139386 [2409.08002].

[19] J. Bulava, F. Knechtli, V. Koch, C. Morningstar and M. Peardon, *The quark-mass dependence of the potential energy between static colour sources in the QCD vacuum with light and strange quarks*, *Phys. Lett. B* **854** (2024) 138754 [2403.00754].

[20] J. Bulava, B. Hörz, F. Knechtli, V. Koch, G. Moir, C. Morningstar et al., *String breaking by light and strange quarks in QCD*, *Phys. Lett. B* **793** (2019) 493 [1902.04006].

[21] Particle Data Group collaboration, *Review of particle physics*, *Phys. Rev. D* **110** (2024) 030001.

[22] N. Brambilla, A. Mohapatra, T. Scirpa and A. Vairo, *Nature of χc1(3872) and Tcc+(3875)*, *Phys. Rev. Lett.* **135** (2025) 131902 [2411.14306].

[23] R. Bruschini, *Why quarkonium hybrid coupling to two S-wave heavy-light mesons is not suppressed*, *Phys. Rev. D* **109** (2024) L031501 [2306.17120].

[24] J. Tarrús Castellà, *Effect of continuum states on the double-heavy hadron spectra*, *JHEP* **06** (2024) 107 [2401.13393].

[25] E. Braaten and R. Bruschini, *Model-independent predictions for decays of hidden-heavy hadrons into pairs of heavy hadrons*, *Phys. Rev. D* **109** (2024) 094051 [2403.12868].

[26] N. Brambilla, A. Mohapatra and A. Vairo, *Unraveling pentaquarks with the Born-Oppenheimer effective theory*, *Phys. Rev. D* **112** (2025) 114037 [2508.13050].

[27] LHCb collaboration, *Observation of an exotic narrow doubly charmed tetraquark*, *Nature Phys.* **18** (2022) 751 [2109.01038].

[28] LHCb collaboration, *Study of the doubly charmed tetraquark* T_{cc}^+, *Nature Commun.* **13** (2022) 3351 [2109.01056].

[29] Y. Lyu, S. Aoki, T. Doi, T. Hatsuda, Y. Ikeda and J. Meng, *Doubly Charmed Tetraquark Tcc+ from Lattice QCD near Physical Point*, *Phys. Rev. Lett.* **131** (2023) 161901 [2302.04505].

[30] P. Bicudo, M. Krstic Marinkovic, L. Müller and M. Wagner, *Antistatic-antistatic* $\bar{Q}\bar{Q}qq$ *potentials for u, d and s light quarks from lattice QCD*, in *41st International Symposium on Lattice Field Theory*, 9, 2024, 2409.10786.

[31] LHCb collaboration, *Observation of* $J/\psi p$ *Resonances Consistent with Pentaquark States in* $\Lambda_b^0 \to J/\psi K^- p$ *Decays*, *Phys. Rev. Lett.* **115** (2015) 072001 [1507.03414].

[32] LHCb collaboration, *Observation of a narrow pentaquark state,* $P_c(4312)^+$*, and of two-peak structure of the* $P_c(4450)^+$, *Phys. Rev. Lett.* **122** (2019) 222001 [1904.03947].

[33] N. Brambilla, M. Butenschoen, S. Hibler, A. Mohapatra, A. Vairo and X. Wang, *Inclusive hadroproduction of* $\chi_{c1}(3872)$*,* X_b *and pentaquarks*, 2602.14916.